Extending the C+L System Bandwidth versus Exploiting Part of the S-band: Network Capacity and Interface Count Comparison

Extending the C+L System Bandwidth versus Exploiting Part of the S-band: Network Capacity and Interface Count Comparison

Rasoul Sadeghi[(1)], Bruno Correia[(1)], Nelson Costa[(2)], João Pedro[(2, 3)], Antonio Napoli[(4)], and Vittorio Curri[(1)]

[(1)] Politecnico di Torino, Torino, Italy rasoul.sadeghi@polito.it [(2)] Infinera Unipessoal Lda, Carnaxide, Portugal [(3)] Instituto de Telecomunicações, Instituto Superior Técnico, Lisboa, Portugal [(4)] Infinera, Munich, Germany

Abstract *In this work, the network capacity and device count (amplifiers and interfaces) are investigated for different multi-band approaches, highlighting the trade-off between exploiting part of the S-band and extending C+L-band systems. ©2022 The Author(s)*

Introduction

The continuous growth of IP traffic demand over the years pushed network service providers to enhance the available network capacity while keeping network costs and power consumption under control. Accordingly, multi-band transmission (MBT) optical networking is considered as a feasible solution to cost-effectively expand wavelength-division multiplexing (WDM) network capacity[1],[2]. The target of MBT is to increase the bandwidth of WDM systems from ≈ 4.8 THz of the C-band to include the L-band and other bands up to ≈ 50 THz, using the entire low-loss single-mode spectrum of widely-deployed ITU-T G.652.D optical fibers infrastructure[3],[4]. This approach requires dedicated amplifiers for each band. Another possibility to augment fiber capacity is to extend the used bandwidth of traditional bands (C and L) from 4.8 to approximately 6 THz in each band[5], without needing new amplifiers. Additionally, a network enforcing traffic grooming enables to increase network capacity by operating transceivers (TRXs) at higher order modulation formats[6],[7]. Particularly, a lightpath (LP) between source and destination is divided into several shorter transparent segments via optical-electrical-optical (OEO) signal regeneration at intermediate nodes using a pair of standard TRXs, such as Open400ZR+[8], improving the spectral efficiency of the provisioned LPs. Several works have shown the benefits of signal regeneration (translucent design) to augment network capacity[9],[10].

In this work, we compare different strategies to enhance the overall network capacity, while also considering the number of required interfaces. The paper is organized as follows. In section Methodology and Metrics, the quality of transmission (QoT) evaluation method is described. Moreover, we detail the upgrade scenarios analyzed in terms of bandwidth and, consequently, number of available channels. The methodology employed for network design and evaluation and the key simulation results for transparent and translucent design are presented in section Network Analysis Description and Results for four different investigated MBT scenarios. Finally, the main conclusions of this work are outlined in section Conclusions.

Methodology and Metrics

The QoT metric used in this work is the generalized signal-to-noise ratio (GSNR), which includes both amplified spontaneous emission (ASE) noise and nonlinear interference (NLI) generation[11]. Moreover, in order to properly compute the NLI contribution, and its interaction with the stimulated Raman scattering (SRS), in scenarios with such wide bandwidth, we made use of the generalized Gaussian noise (GGN)[12]–[14]. All simulations in this work have a WDM grid spacing of 75 GHz and a symbol rate of 64 Gbaud. The scenarios simulated are: (a) regular C+L and C+L+S1, each band supporting 64 WDM channels with a bandwidth of 4.8 THz each; (b) super C and C+L, consisting of 80 channels for each band, where their bandwidth is considered to be ≈ 6 THz. To be more precise, regular C- and L-band frequency range is $\{$191.31-196.03$\}$ THz and $\{$186.08-190.81$\}$ THz, respectively. These values are expanded to $\{$190.7-196.625$\}$ THz for the super C-band and $\{$184.27-190.2$\}$ THz for the super L-band[15]. Moreover, the frequency range of the S1-band is $\{$196.53-201.26$\}$ THz. We combine all these four scenarios with two network design strategies: (1) complete end-to-end transparency; (2) possible assignment of 3R regenerator at intermediate nodes[7]. Following a disaggregated approach, the total path GSNR of a request (consisting of several spans) can be computed based on the GSNR of each span. The single-span GSNR profile of 75 km for all scenarios in (a) and (b) are presented in Fig. 1. This figure consists of the GSNR profile of four MBT scenarios namely C+L- (blue), C+L+S1- (green), super C- (black), and super C+L-band (red). The bandwidth of regular bands is marked with the dashed gray line on the bottom x-axis, and the expanded bands are marked with the dashed red line on the top x-axis. In this work, the noise figure (NF) values for all bands are the same as in ref.[7], although for the super bands these values are interpolated for the proper frequency ranges. According to this figure, the average GSNR value in the super C-band only is equal to

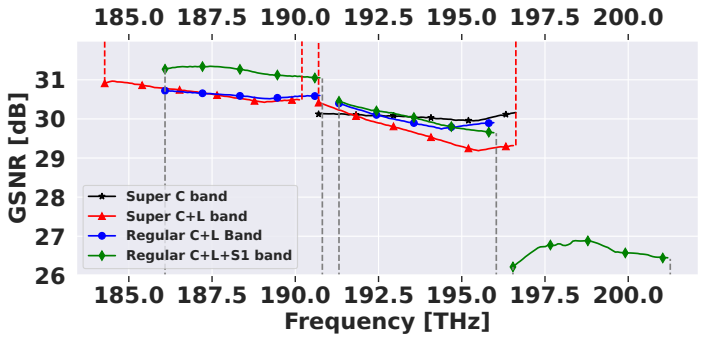

Fig. 1: GSNR profile in a single span of 75 km.

30 dB. On one hand, the average GSNR value for the C- and L-band is equal to 29.9 and 30.6 dB in the regular C+L-band scenario. On the other hand, the GSNR value in the super C-band decreased to 29.6 dB in the super C+L-band scenario, whereas the super L-band GSNR value remained almost equal with respect to regular L-band, that is, 30.6 dB. In the Super C+L scenario, the C-band presents a degradation if compared to the super C-band only, due to the higher amount of channels in both bands, which causes extra power loss. These values in the C+L+S1-band scenario are equal to 30, 31.2, and 26.6 dB for the C-, L-, and S1-band, respectively.

Network Analysis Description and Results

In this section, the results of network performance in regular and super MBT scenarios are presented and discussed. The network analysis considers the US-NET[7] topology, which comprises 24 nodes and 43 links with an average link length of 308 km. Moreover, we assume OpenZR+ TRX[8] supporting three dual-polarization modulation formats, each having a specific required GSNR (RGSNR) and power consumption. The RGSNR in back-to-back operation (B2B) for each modulation format is indicated in[16]. The Statistically Network Assessment Process (SNAP), which is a Monte Carlo (MC) based procedure, has been used to evaluate the network performance. Progressive traffic loading[17] is enforced with traffic requests of 100 Gb/s. The analysis focuses on comparing regular C+L, C+L+S1, super C, and super C+L bands in transparent and translucent network designs. In the transparent network design, the highest feasible modulation format is selected by SNAP according to the QoT of the end-to-end LP. However, in the translucent network design, the LP can be divided in the minimum number of sub-paths whose QoT allows to support the most spectral efficient modulation format possible (using Algorithm 1 in ref[7]). This method increases the network capacity, while deploying the minimum number of extra interfaces. For simplicity, wavelength conversion is not considered after each signal regeneration. The k-shortest path algorithm is used to determine the five shortest paths between every source and destination node pairs.

Fig. 2 shows the total allocated traffic for different blocking probabilities (BPs) considering transparent (solid lines) and translucent (dashed lines) MBT scenarios. According to Fig. 2a, it is observable that in all scenarios 3R regenerator assignment (i.e., translucent network design) leads to capacity increases when compared to transparent network design. In the transparent and translucent super C-band (80 channels), the total allocated traffic for a BP=10^{-2} is equal to 130 and 150 Tb/s, respectively. Network capacity in the C+L-band with 128 channels in total is equal to 254 Tb/s in the transparent network design; this value increases to 287 Tb/s at the expense of extra regenerators in the translucent network design. The C- and L-band bandwidth widening (super C+L-band with a total of 160 channels) leads to an increase in capacity to 332 Tb/s with transparent network design and to 379 Tb/s with translucent network design. Importantly, not only the delivered traffic at the super C+L-band (160 channels), in both transparent and translucent, is significantly higher than that with transparent and translucent C+L-band (128 channels), but also this value in the translucent super C+L-band (160 channels) almost matches that with the transparent C+L+S1-band (192 channels). In both cases (dashed red curve and solid green curve) the capacity supported for the referred blocking probability is almost equal to 375 Tb/s. As expected, the scenario offering the highest capacity is the translucent C+L+S1 (dashed green curve), since it combines the use of more bands and additional TRXs to improve spectral efficiency. Particularly, the total allocated traffic is 458 Tb/s at a BP of 1%. To gain further insight, the multiplicative factor (MF) of allocated traffic for all investigated scenarios mentioned is illustrated in Fig. 2b for a BP of 1% and using the transparent super C-band as the baseline. This figure shows that the 3R regenerator assignment increases the network capacity by only 15% in the case of super C-band only. Exploiting the super L-band with an already deployed super C-band leads to an increase in the

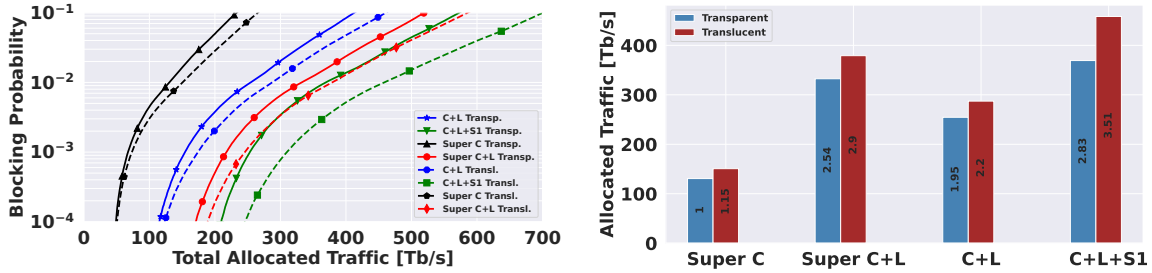

(a) (b)

Fig. 2: (a) Total allocated traffic for different BPs and (b) total allocated traffic for different MBT network designs at the BP of 1%. The MF is indicated for each case.

Tab. 1: Interface count, bit rate per interface, and number of deployed optical amplifiers at the delivered traffic of 250 Tb/s.

Traffic=250 Tbps	Interfaces Count	Bit rate/Interface [Gb/s/interface]	Amp. Count
Transp. Super C	1572	159	173
Transp. Super C+L	1714	146	346
Transp. C+L	1702	147	346
Transp. C+L+S1	1732	144	519
Transl. Super C	1884	132	173
Transl. Super C+L	1970	127	346
Transl. C+L	1960	127	346
Transl. C+L+S1	2185	114	519

network capacity of $\times$2.54 times in the transparent network design. This increase is higher than that allowed by both regular C+L-band transparent and translucent network designs, which are $\times$1.95 and $\times$2.2 times higher in comparison to the super C-band, respectively. Translucent C+L+S1-band gives the highest MF, $\times$3.51 times, among all investigated scenarios. But it is important to notice that the MF of network capacity is almost the same, i.e., $\times$2.9 times, in the translucent super C+L-band and transparent C+L+S1-band.

In order to assess the potential of the different configurations, it is also critical to estimate the cost associated to each capacity increase strategy. With this aim, Table 1 provides the number of used interfaces (i.e., TRXs) and the bit-rates per interface for each scenario for an allocated traffic of 250 Tb/s. At a glance, this table shows that not only increasing the number of wavelengths lead to a rise in the used number of interfaces, but also this amount grows in the translucent network design in comparison to the transparent network design. For example, the interface count in the transparent super C-band is equal to 1572, however, this value in the translucent network designs of the super C-band is equal to 1884. The number of used interfaces in the transparent super C+L-band and regular C+L-band is almost the same, 1714 and 1702, respectively. However, as seen previously, transparent super C+L-band can be used to further scale network capacity when compared to transparent regular C+L-band (Fig. 2a). Moreover, not only the transparent super C+L-band has a better performance in terms of capacity than the translucent regular C+L-band (Fig. 2a), but it also demands fewer interfaces than the latter strategy (which requires 1960 interfaces to support 250 Tb/s). According to Fig. 2a, network capacity in the translucent super C+L-band is almost equal to the transparent regular C+L+S1-band; however, the number of used interfaces in the translucent super C+L-band, 1970 interfaces, is higher than transparent regular C+L+S1-band, 1732 interfaces, for the same delivered traffic of 250 Tb/s. Noteworthy, Tab. 1 also shows the number of deployed amplifiers in each investigated scenario are provided. As can be seen, with the same amount of deployed amplifiers, 346 in the regular and super C+L-band cases, the bit-rate per-interface value in the transparent super C+L-band is higher than the translucent regular C+L-band case (146 versus 127 Gb/s/interface). But the bit-rate per-interface value in the translucent super C+L-band (with 346 amplifiers) is less than the transparent regular C+L+S1-band (with 519 amplifiers) scenario which is 127 and 144 Gb/s/interface. Overall, translucent super C+L-band provides similar maximium capacity to transparent C+L+S1-band and for a target capacity of 250 Tb/s requires 238 more TRXs but avoids deploying additional 173 amplifiers.

Conclusions

In this work, we compared the network capacity as well as the number of interfaces between regular and extended bandwidth bands in transparent and translucent network designs. We showed that super bands lead to an increase in network capacity in comparison to the regular bands for the same number of bands. Importantly, super C+L-band translucent network design provides the same delivered traffic compared with regular C+L+S1-band transparent network design, with both solutions featuring a trade-off between extra interfaces and extra amplifiers.

Acknowledgements

This project has received funding from the European Union Horizon 2020 research and innovation program under the Marie Skłodowska-Curie WON project, grant agreement 814276, and the B5G-OPEN project, grant agreement 101016663.

References

[1] F. Hamaoka, M. Nakamura, S. Okamoto, *et al.*, "Ultra-wideband wdm transmission in s-, c-, and l-bands using signal power optimization scheme," *Journal of Lightwave Technology*, vol. 37, no. 8, pp. 1764–1771, 2019.

[2] R. Sadeghi, B. Correia, E. Virgillito, *et al.*, "Optimal spectral usage and energy efficient s-to-u multiband optical networking," in *Optical Fiber Communication Conference (OFC) 2022*, Optica Publishing Group, 2022, W3F.7. DOI: 10.1364/OFC.2022.W3F.7. [Online]. Available: http://opg.optica.org/abstract.cfm?URI=OFC-2022-W3F.7.

[3] A. Ferrari, E. Virgillito, and V. Curri, "Band-division vs. space-division multiplexing: A network performance statistical assessment," *Journal of Lightwave Technology*, vol. 38, no. 5, pp. 1041–1049, 2020.

[4] R. Sadeghi, B. Correia, E. Virgilito, *et al.*, "Optimized translucent s-band transmission in multi-band optical networks," in *2021 European Conference on Optical Communication (ECOC)*, 2021, pp. 1–4. DOI: 10.1109/ECOC52684.2021.9605809.

[5] J. Pedro, N. Costa, and S. Sanders, "Cost-effective strategies to scale the capacity of regional optical transport networks," *Journal of Optical Communications and Networking*, vol. 14, no. 2, A154–A165, 2022.

[6] G. Zhang, M. De Leenheer, and B. Mukherjee, "Optical traffic grooming in ofdm-based elastic optical networks," *Journal of Optical Communications and Networking*, vol. 4, no. 11, B17–B25, 2012.

[7] R. Sadeghi, B. Correia, A. Souza, *et al.*, "Transparent vs translucent multi-band optical networking: Capacity and energy analyses," *Journal of Lightwave Technology*, pp. 1–1, 2022. DOI: 10.1109/JLT.2022.3167908.

[8] *Open ZR+ MSA Technical Specification*, https://openzrplus.org/site/assets/files/1075/openzrplus_1p0.pdf.

[9] Y. Jiang, Q. Chen, Y. Lei, Q. Zhang, and B. Chen, "Energy efficiency with minimized-regenerators placement in ip-over-flexible bandwidth optical networks," in *2019 18th International Conference on Optical Communications and Networks (ICOCN)*, 2019, pp. 1–3. DOI: 10.1109/ICOCN.2019.8934140.

[10] M. Kanj, E. L. Rouzic, J. Meuric, and B. Cousin, "Optical power control in translucent flexible optical networks with GMPLS control plane," *J. Opt. Commun. Netw.*, vol. 10, no. 9, pp. 760–772, Sep. 2018. DOI: 10.1364/JOCN.10.000760. [Online]. Available: http://www.osapublishing.org/jocn/abstract.cfm?URI=jocn-10-9-760.

[11] M. Filer, M. Cantono, A. Ferrari, G. Grammel, G. Galimberti, and V. Curri, "Multi-vendor experimental validation of an open source qot estimator for optical networks," *J. Lightwave Technol.*, vol. 36, no. 15, pp. 3073–3082, Aug. 2018. [Online]. Available: http://jlt.osa.org/abstract.cfm?URI=jlt-36-15-3073.

[12] M. Cantono, D. Pilori, A. Ferrari, *et al.*, "On the interplay of nonlinear interference generation with stimulated Raman scattering for QoT estimation," *Journal of Lightwave Technology*, vol. 36, no. 15, pp. 3131–3141, 2018.

[13] D. Semrau, R. I. Killey, and P. Bayvel, "The Gaussian noise model in the presence of inter-channel stimulated raman scattering," *Journal of Lightwave Technology*, vol. 36, no. 14, pp. 3046–3055, Jul. 2018, ISSN: 0733-8724.

[14] A. D'Amico, B. Correia, E. London, *et al.*, "Scalable and disaggregated ggn approximation applied to a c+l+s optical network," *Journal of Lightwave Technology*, pp. 1–1, 2022.

[15] *Super C+L band*, https://www-file.huawei.com/-/media/corporate/pdf/white%20paper/ovum-spectrum-and-amplification.pdf?la=en.

[16] J. Pedro and S. Pato, "Capacity increase and hardware savings in dwdm networks exploiting next-generation optical line interfaces," pp. 1–6, 2018.

[17] V. Curri, M. Cantono, and R. Gaudino, "Elastic All-Optical Networks: A New Paradigm Enabled by the Physical Layer. How to Optimize Network Performances?" *Journal of Lightwave Technology*, vol. 35, no. 6, pp. 1211–1221, 2017, ISSN: 0733-8724. DOI: 10.1109/JLT.2017.2657231.